Periodicity property of relativistic Thomson scattering with application to exact calculations of angular and spectral distributions of the scattered field

Alexandru Popa*

National Institute for Laser, Plasma and Radiation Physics, Laser Department, P.O. Box MG-36, Bucharest, RO-077125, Romania

(Received 14 February 2011; published 16 August 2011)

We prove that the analytical expression of the intensity of the relativistic Thomson scattered field for a system composed of an electron interacting with a plane electromagnetic field can be written in the form of a composite periodic function of only one variable, that is, the phase of the incident field. This property is proved without using any approximation in the most general case in which the field is elliptically polarized, the initial phase of the incident field and the initial velocity of the electron are taken into consideration, and the direction in which the radiation is scattered is arbitrary. This property leads to an exact method for calculating the angular and spectral distributions of the scattered field, which reveals a series of physical details of these distributions, such as their dependence on the components of the initial electron velocity. Since the phase of the field is a relativistic invariant, it follows that the periodicity property is also valid when the analysis is made in the inertial system in which the initial velocity of the electron is zero in the case of interactions between very intense electromagnetic fields and relativistic electrons. Consequently, the calculation method can be used for the evaluation of properties of backscattered hard radiations generated by this type of interaction. The theoretical evaluations presented in this paper are in good agreement with the experimental data from literature.

DOI: 10.1103/PhysRevA.84.023824 PACS number(s): 42.65.Ky, 03.50.−z, 52.25.Os

I. INTRODUCTION

Important nonlinear interactions between fields and particles were predicted theoretically in the early years of lasers, even when laser intensities were too small to allow experimental studies of these interactions [1–3]. Starting in the 1970s, due to the development of high-power lasers, a large number of both theoretical and experimental papers analyzed these interactions, most notably the nonlinear Thomson scattering [4–16]. More recently, the emergence of ultraintense laser pulses, characterized by beam intensities higher than 10^{18} W cm^{-2}, led to increased interest in this area of research since nonlinear Thomson scattering opened up the possibility of high-brightness hard-x-ray production using lasers [17–24]. Concurrently, the same physical phenomenon was analyzed in complementary papers as Compton scattering [25–30].

The majority of the nonlinear Thomson scattering approaches presented in literature are based on relativistic solutions to the equations of motion of the electrons involved, which lead to expressions for the electrons' velocities and accelerations. These expressions are then introduced in the equations of the energy radiated per solid angle and per unit frequency interval corresponding to an arbitrary direction, namely, Eqs. (14.60) and (14.67) from Jackson's book on classical electrodynamics [31], which are deduced from Fourier transforms of the Liènard-Wiechert relation. For example, Refs. [4,6,8–12,14–16] use Eq. (14.67), the treatment from Ref. [7] is a continuation of that from Ref. [4], and Ref. [5] uses (14.60). On the other hand, Ref. [13] uses an expression for the angular distribution, which is derived by the summation of harmonics in the spectral and angular distribution, as it results in quantum electrodynamics [32]. A disadvantage of calculating the intensities of the scattered radiation harmonics based on Eqs. (14.60) and (14.67) from Ref. [31] is the fact that this method leads to infinite sums of Bessel functions. This issue is analyzed in Ref. [4], which shows that the general result for the nth harmonic scattering can not usually be expressed in a tractable form. For this reason, certain approximations are imposed in the frame of this method such as, for example, the approximation which led from Eq. (29) to Eq. (33) in Ref. [10].

In this paper, we propose a different approach, which is based on the observation that the velocity and acceleration of the electron are periodic functions of the phase of the electromagnetic wave. This property results rigorously from the equations describing the electron motion in the most general case in which the electromagnetic field is elliptically polarized and the initial phase of the field and the initial components of the electron velocity are taken into account. Currently, the techniques for solving these equations are very well known [33]. Since the velocity and acceleration of the electron enter in the Liènard-Wiechert relation, which gives the intensity of the scattered field, it follows that this intensity and the intensity of the scattered beam in an arbitrary direction are periodic functions of only one variable, namely, the phase of the incident electromagnetic field. Due to the periodicity, the spectrum of the scattered radiation is obtained by a Fourier series expansion of the scattered field expression. The result is that the frequency of the fundamental component of the spectrum is identical to the frequency of the incident field. It follows that the intensity of the scattered radiation and its harmonics can be expressed in the analytic form of simple composite functions of one variable, which can be calculated by simple computer programs. Since the phase of the field is a relativistic invariant, it follows that our approach is valid in the case of interactions between very intense electromagnetic fields and relativistic electrons when the analysis is made in the inertial system in which the initial velocity of the electron is zero. Due to the periodicity property, our treatment leads to the existence of harmonics of the backscattered beam frequency. This result has been recently confirmed experimentally [34].

*ampopa@rdslink.ro

The profile of the backscattered beam and its energy result accurately.

In order to verify the accuracy of the calculation method, we calculate typical angular and spectral distributions of the scattered field and compare them with numerous reliable theoretical and experimental data from literature. In the same time, we show that the method, due to its accuracy, can be useful for the study of new physical details, such as, for example, the influence of the values of the electron initial velocity components on angular and spectral distributions of the scattered radiation.

Remarkably, the relations used to demonstrate periodicity are useful also for revealing new properties of the system. In this respect, we prove that the divergence of the energy-momentum four-vector is zero in the general case for the system analyzed in this paper. It follows that, by virtue of a property proven by Motz and Selzer [35], the Klein-Gordon equation written for our system is verified exactly by the wave function associated to the classical motion of the electron. This result is an explanation for the accuracy of the classical treatment presented in our paper.

The paper is structured as follows. In Sec. II, we demonstrate the periodicity of the electron velocity and acceleration, and also the periodicity of the intensity of the electric scattered field. This analysis leads to the algorithm used to calculate the average intensity of the scattered field and the average harmonics intensities. For completeness, we present a justification of the classical treatment. We present physical details of the angular and spectral distributions of the scattered beam, which result from theory and are confirmed by experimental data from literature. We show that the calculations reveal an influence of initial electron velocity on these distributions. In Sec. III, we calculate the properties of the backscattered radiation in the case of the interaction between very intense electromagnetic beams and relativistic electrons when the analysis is made in the system in which the electron velocity is zero. The equations are written in the International System.

II. PERIODICITY PROPERTIES OF THE THOMSON SCATTERED BEAM

A. Initial data

We analyze a system composed of an electron interacting with a very intense electromagnetic elliptically polarized plane field of a laser beam. We consider the following initial hypotheses:

(h1) In a Cartesian system of coordinates, the intensity of the electric field and of the magnetic induction vector, denoted, respectively, by $\overline{E}_L$ and $\overline{B}_L$, are polarized in the plane xy, while the wave vector, denoted by $\overline{k}_L$, is parallel to the axis oz. The expression of the electric field is

$$\overline{E}_L = E_{M1}\cos\eta\,\overline{i} + E_{M2}\sin\eta\,\overline{j} \tag{1}$$

with

$$\eta = \omega_L t - |k_L| z + \eta_i \quad \text{and} \quad |k_L| c = \omega_L, \tag{2}$$

where $\overline{i}$, $\overline{j}$, and $\overline{k}$ are versors of the ox, oy, and oz axes, E_{M1} and E_{M2} are the amplitudes of the electric field oscillations in the ox and oy directions, ω_L is the angular frequency of the laser electromagnetic field, c is the light velocity, η_i is an arbitrary initial phase, and t is the time in the xyz system in which the motion of the electron is studied.

From the properties of the electromagnetic field, it follows that the corresponding magnetic induction vector is

$$\overline{B}_L = -B_{M2}\sin\eta\,\overline{i} + B_{M1}\cos\eta\,\overline{j} \tag{3}$$

with

$$E_{M1} = cB_{M1}, \quad E_{M2} = cB_{M2}, \quad \text{and} \quad c\overline{B}_L = \overline{k}\times\overline{E}_L, \tag{4}$$

where B_{M1} and B_{M2} are the amplitudes of the magnetic field oscillations in the oy and ox directions.

(h2) We consider the following initial conditions in the most general case when the components of the electron velocities, denoted by v_x, v_y, and v_z, have arbitrary values:

$$\begin{aligned} &t = 0, \quad x = y = z = 0, \quad v_x = v_{xi}, \\ &v_y = v_{yi}, \quad v_z = v_{zi}, \quad \text{and} \quad \eta = \eta_i. \end{aligned} \tag{5}$$

(h3) Since the "acceleration-field" component in the Lièнard-Wiechert relation is related to the electromagnetic wave radiated by the particle [36], the intensity of the electric field generated by the electron motion is given by the relation

$$\overline{E} = \frac{-e}{4\pi\varepsilon_0 cR}\frac{\overline{n}\times[(\overline{n}-\overline{\beta})\times\dot{\overline{\beta}}]}{(1-\overline{n}\cdot\overline{\beta})^3}. \tag{6}$$

Here, e is the absolute value of the electron charge, ε_0 is the vacuum permittivity, $\overline{\beta} = \overline{v}/c$, where $\overline{v}$ is the electron velocity, R is the distance from the electron to the observation point (the detector), and $\overline{n}$ is the versor of the direction electron detector. The dot in $\dot{\overline{\beta}}$ signifies derivation with respect to time. By virtue of the significance of the quantities entering in the Lièнard-Wiechert equation, it results that the field $\overline{E}$ corresponds to the time $t + R/c$ and we have $\overline{E} = \overline{E}(\overline{r} + R\overline{n}, t + R/c)$, where $\overline{r}$ is the position vector of the electron with respect to a system having its origin at the point defined by (5). The relation $R \gg r$ is overwhelmingly fulfilled [31].

By using spherical coordinates for which θ is the azimuthal angle between the $\overline{n}$ and $\overline{k}$ versors and ϕ is the polar angle in the plane xy, the versor $\overline{n}$ can be written as

$$\overline{n} = \sin\theta\cos\phi\,\overline{i} + \sin\theta\sin\phi\,\overline{j} + \cos\theta\,\overline{k}. \tag{7}$$

Taking into account Eqs. (1) and (3), the equations of motion of the electron are

$$m\frac{d}{dt}(\gamma v_x) = -eE_{M1}\cos\eta + ev_z B_{M1}\cos\eta, \tag{8}$$

$$m\frac{d}{dt}(\gamma v_y) = -eE_{M2}\sin\eta + ev_z B_{M2}\sin\eta, \tag{9}$$

$$m\frac{d}{dt}(\gamma v_z) = -ev_x B_{M1}\cos\eta - ev_y B_{M2}\sin\eta, \tag{10}$$

where

$$\gamma = \left(1-\beta_x^2-\beta_y^2-\beta_z^2\right)^{-\frac{1}{2}} \tag{11}$$

with $\beta_x = v_x/c$, $\beta_y = v_y/c$, and $\beta_z = v_z/c$.

Using Eq. (4), the equations of motion become

$$\frac{d}{dt}(\gamma\beta_x) = -a_1\omega_L(1-\beta_z)\cos\eta, \tag{12}$$

$$\frac{d}{dt}(\gamma\beta_y) = -a_2\omega_L(1-\beta_z)\sin\eta, \tag{13}$$

$$\frac{d}{dt}(\gamma\beta_z) = -\omega_L(a_1\beta_x\cos\eta + a_2\beta_y\sin\eta), \tag{14}$$

where

$$a_1 = \frac{eE_{M1}}{mc\omega_L} \quad \text{and} \quad a_2 = \frac{eE_{M2}}{mc\omega_L} \tag{15}$$

are relativistic parameters.

From this point on, no approximation is being made in order to solve the equation system comprised of Eqs. (6), (12), (13), and (14).

B. Periodicity properties of $\bar{\beta}$ and $\dot{\bar{\beta}}$

We calculate first β_x, β_y, β_z, $\dot{\beta}_x$, $\dot{\beta}_y$, and $\dot{\beta}_z$, which are necessary in our analysis. We multiply Eqs. (12), (13), and (14), respectively, by β_x, β_y, and β_z. Taking into account that $\beta_x^2+\beta_y^2+\beta_z^2 = 1-1/\gamma^2$, their sum leads to

$$\frac{d\gamma}{dt} = -\omega_L(a_1\beta_x\cos\eta + a_2\beta_y\sin\eta). \tag{16}$$

From (14) and (16), we obtain $d(\gamma\beta_z)/dt = d\gamma/dt$. We integrate this relation with respect to time between 0 and t, taking into account the initial conditions (5), and obtain $\gamma-\gamma_i = \gamma\beta_z - \gamma_i\beta_{zi}$. Using (2), we have

$$1-\beta_z = \frac{1}{\omega_L}\frac{d\eta}{dt} = \frac{f_0}{\gamma} \tag{17}$$

with

$$f_0 = \gamma_i(1-\beta_{zi}), \tag{18}$$

where $\beta_{xi} = v_{xi}/c$, $\beta_{yi} = v_{yi}/c$, $\beta_{zi} = v_{zi}/c$, and $\gamma_i = 1/\sqrt{1-\beta_{xi}^2-\beta_{yi}^2-\beta_{zi}^2}$.

We integrate (12) with respect to time between 0 and t, taking into account (17) and the initial conditions (5) and obtain

$$\gamma\beta_x - \gamma_i\beta_{xi} = -a_1(\sin\eta - \sin\eta_i) \tag{19}$$

or

$$\beta_x = \frac{f_1}{\gamma}, \tag{20}$$

where

$$f_1 = f_1(\eta) = -a_1(\sin\eta - \sin\eta_i) + \gamma_i\beta_{xi}. \tag{21}$$

Similarly, by integrating (13) and taking into account (5) and (17), we obtain

$$\beta_y = \frac{f_2}{\gamma}, \tag{22}$$

where

$$f_2 = f_2(\eta) = -a_2(\cos\eta_i - \cos\eta) + \gamma_i\beta_{yi}. \tag{23}$$

We substitute the expressions of β_x, β_y, and β_z, respectively, from Eqs. (20), (22), and (17) into (11) and obtain the expression of γ:

$$\gamma = \gamma(\eta) = \frac{1}{2f_0}\left[1+f_0^2+f_1^2+f_2^2\right]. \tag{24}$$

From (17), we obtain

$$\beta_z = \frac{f_3}{\gamma}, \tag{25}$$

where

$$f_3 = f_3(\eta) = \gamma - f_0. \tag{26}$$

From (16), (20), and (22), we have also

$$\frac{d\gamma}{dt} = -\frac{\omega_L}{\gamma}(a_1f_1\cos\eta + a_2f_2\sin\eta). \tag{27}$$

From Eq. (12), we obtain $\dot{\beta}_x$:

$$\dot{\beta}_x = -\frac{1}{\gamma}\left[\beta_x\frac{d\gamma}{dt} + a_1\omega_L(1-\beta_z)\cos\eta\right]. \tag{28}$$

By introducing in (28) the expressions of β_x, β_z, and $d\gamma/dt$, respectively, from (20), (17), and (27), we obtain

$$\dot{\beta}_x = \omega_L g_1, \tag{29}$$

where

$$g_1 = g_1(\eta) = -\frac{a_1f_0}{\gamma^2}\cos\eta + \frac{f_1}{\gamma^3}(a_1f_1\cos\eta + a_2f_2\sin\eta). \tag{30}$$

Similarly, from (13) and (14), we obtain $\dot{\beta}_y$ and $\dot{\beta}_z$:

$$\dot{\beta}_y = \omega_L g_2, \tag{31}$$

where

$$g_2 = g_2(\eta) = -\frac{a_2f_0}{\gamma^2}\sin\eta + \frac{f_2}{\gamma^3}(a_1f_1\cos\eta + a_2f_2\sin\eta) \tag{32}$$

and

$$\dot{\beta}_z = \omega_L g_3, \tag{33}$$

where

$$g_3 = g_3(\eta) = -\frac{f_0}{\gamma^3}(a_1f_1\cos\eta + a_2f_2\sin\eta). \tag{34}$$

We observe that, from (21) and (23), it follows that f_1 and f_2 are periodic functions of only one variable, that is, η. By virtue of this property, from (24) and (26), it follows that γ and f_3 are also periodic functions of η. Taking into account these relations, from (30), (32), and (34), it results that g_1, g_2, and g_3 are periodic functions of η. Finally, from (20), (22), (25), (29), (31), and (33), it follows, respectively, that β_x, β_y, β_z, $\dot{\beta}_x$, $\dot{\beta}_y$, and $\dot{\beta}_z$ are periodic functions of only one variable η.

The above relations are written in the general case of an elliptically polarized field when the constants η_i, β_{xi}, β_{yi}, and β_{zi} are arbitrary. These relations can be written for the motion of the electron in a circularly polarized field, substituting $E_{M1} = E_{M2}$, $B_{M1} = B_{M2}$, and $a_1 = a_2$. Also, these relations can be written in the case of a linearly polarized field when $E_{M2} = 0$, $B_{M2} = 0$, and $a_2 = 0$.

The above relations are valid during the entire duration of the laser pulse. At the end of the pulse, the values of E_{M1} and E_{M2} decrease to zero in a very short period of time. We note this by $E_{M1} \to 0$ and $E_{M2} \to 0$. From (15), it follows that $a_1 \to 0$ and $a_2 \to 0$, and from (21) and (23), it follows that $f_1 \to \gamma_i \beta_{xi}$ and $f_2 \to \gamma_i \beta_{yi}$. By virtue of (18), (20), and (24), we have $\beta_x \to 2\gamma_i(1-\beta_{zi})(\gamma_i\beta_{xi})/[1+\gamma_i^2(1-\beta_{zi})^2+(\gamma_i\beta_{xi})^2+(\gamma_i\beta_{yi})^2]$. It results that, at the end of the laser pulse, when $E_{M1} \to 0$ and $E_{M2} \to 0$, a simple calculation leads to $\beta_x \to \beta_{xi}$. A similar calculation shows that $\beta_y \to \beta_{yi}$ and $\beta_z \to \beta_{zi}$. Consequently, after the interaction with the laser field, the total energy transferred from the electromagnetic field to the electron is zero. Remarkably, this conclusion holds also if the interaction between the electromagnetic field and a free electron is analyzed in the frame of the quantum electrodynamics. Indeed, Sec. 4.1 of Ref. [37] shows that, by virtue of the momentum conservation law, the electrons can neither emit nor absorb a free photon in such systems. Therefore, after the interaction, the kinetic energy of the electron remains unchanged.

C. Periodicity properties of the electromagnetic field

The periodicity of the scattered electromagnetic field results directly from the Lièнard-Wiechert relation (6), by virtue of the periodicity of $\bar{\beta}$ and $\dot{\bar{\beta}}$. By introducing the components of $\bar{n}$, $\bar{\beta}$, and $\dot{\bar{\beta}}$ from (7), (20), (22), (25), (29), (31), and (33) into (6), we obtain the following expression of the scattered electric field intensity:

$$\bar{E} = \frac{K}{F_1^3}(h_1\bar{i} + h_2\bar{j} + h_3\bar{k}) \text{ with } K = \frac{-e\omega_L}{4\pi\varepsilon_0 cR}, \quad (35)$$

where

$$h_1 = F_2\left(n_x - \frac{f_1}{\gamma}\right) - F_1 g_1, \quad (36)$$

$$h_2 = F_2\left(n_y - \frac{f_2}{\gamma}\right) - F_1 g_2, \quad (37)$$

$$h_3 = F_2\left(n_z - \frac{f_3}{\gamma}\right) - F_1 g_3, \quad (38)$$

and

$$F_1 = 1 - n_x\frac{f_1}{\gamma} - n_y\frac{f_2}{\gamma} - n_z\frac{f_3}{\gamma}, \quad (39)$$

$$F_2 = n_x g_1 + n_y g_2 + n_z g_3, \quad (40)$$

$$n_x = \sin\theta\cos\phi, \ n_y = \sin\theta\sin\phi, \text{ and } n_z = \cos\theta. \quad (41)$$

With the aid of relation (35), we write the intensity of the total scattered radiation as

$$I = c\epsilon_0\bar{E}^2 = c\epsilon_0 K^2\frac{1}{F_1^6}\left(h_1^2 + h_2^2 + h_3^2\right). \quad (42)$$

The average of the intensity of the total scattered radiation, normalized to $c\epsilon_0 K^2$, is denoted by $\underline{I}_{\text{av}}$ and is given by the relation

$$\underline{I}_{\text{av}} = \frac{1}{2\pi}\int_0^{2\pi}\frac{1}{F_1^6}\left(h_1^2 + h_2^2 + h_3^2\right)d\eta. \quad (43)$$

Since the components of the field given by (35) are periodic functions of η, they can be developed in Fourier series, and the expression of the field, normalized to K, becomes

$$\frac{\bar{E}}{K} = f_{1c0}\bar{i} + \left(\sum_{j=1}^{\infty} f_{1sj}\sin j\eta + \sum_{j=1}^{\infty} f_{1cj}\cos j\eta\right)\bar{i} + f_{2c0}\bar{j} + \left(\sum_{j=1}^{\infty} f_{2sj}\sin j\eta + \sum_{j=1}^{\infty} f_{2cj}\cos j\eta\right)\bar{j} + f_{3c0}\bar{k} + \left(\sum_{j=1}^{\infty} f_{3sj}\sin j\eta + \sum_{j=1}^{\infty} f_{3cj}\cos j\eta\right)\bar{k}, \quad (44)$$

where

$$f_{\alpha c0} = \frac{1}{2\pi}\int_0^{2\pi}\frac{h_\alpha}{F_1^3}d\eta; \quad f_{\alpha sj} = \frac{1}{\pi}\int_0^{2\pi}\frac{h_\alpha}{F_1^3}\sin j\eta\, d\eta;$$
$$f_{\alpha cj} = \frac{1}{\pi}\int_0^{2\pi}\frac{h_\alpha}{F_1^3}\cos j\eta\, d\eta \quad (45)$$

with $\alpha = 1,2,3$.

We observe that the quantity

$$\bar{E}_j = \bar{E}_{js} + \bar{E}_{jc}, \quad (46)$$

where

$$\bar{E}_{js} = K(f_{1sj}\bar{i} + f_{2sj}\bar{j} + f_{3sj}\bar{k})\sin j\eta = K(f_{1sj}\bar{i} + f_{2sj}\bar{j} + f_{3sj}\bar{k})\cos j(\eta - \pi/2) \quad (47)$$

and

$$\bar{E}_{jc} = K(f_{1cj}\bar{i} + f_{2cj}\bar{j} + f_{3cj}\bar{k})\cos j\eta \quad (48)$$

is the intensity of the jth harmonic of the electric field. This harmonic is obtained by the addition of two plane fields having phases $j(\eta - \pi/2)$ and $j\eta$ and the same values of the angular frequency and wave-vector magnitude. The latter two are equal, respectively, to $j\omega_L$ and $j|\bar{k}_L|$.

It follows that the angular frequency of the fundamental component of the scattered radiation corresponding to $j = 1$ is identical to the angular frequency of the incident laser field. This result is accurately confirmed by the experimental data presented in Ref. [38], which refers to the relativistic Thomson scattering. That paper shows that the experimental value of the frequency of the fundamental scattered radiation is equal to the laser frequency.

The average of the intensity of the total scattered radiation is denoted by I_{av} and it is given by the relation

$$I_{\text{av}} = \epsilon_0 c\frac{1}{2\pi}\int_0^{2\pi}\bar{E}^2 d\eta. \quad (49)$$

Taking into account (44), (49), and the relations $\int_0^{2\pi}\cos m\eta\cos n\eta\, d\eta = \pi\delta_{mn}$, $\int_0^{2\pi}\sin m\eta\sin n\eta\, d\eta = \pi\delta_{mn}$, and $\int_0^{2\pi}\sin m\eta\cos n\eta\, d\eta = 0$, where m and n are integer numbers, the expression of the average intensity of the total

scattered radiation, normalized to $\epsilon_0 c K^2$, which is denoted by $\underline{I}_{\rm av}$, becomes

$$\underline{I}_{\rm av} = \frac{I_{\rm av}}{\epsilon_0 c K^2} = \frac{1}{2}\sum_{j=1}^{\infty}\left(f_{1sj}^2 + f_{1cj}^2 + f_{2sj}^2 + f_{2cj}^2 + f_{3sj}^2 + f_{3cj}^2\right) + f_{1c0}^2 + f_{2c0}^2 + f_{3c0}^2. \quad (50)$$

The term $f_{1c0}^2 + f_{2c0}^2 + f_{3c0}^2$ in the above relation corresponds to a constant component of the electric scattered field. It reflects the effect of *relativistic rectification*, as it is called by Mourou [39].

The quantity

$$\underline{I}_j = \tfrac{1}{2}\left(f_{1sj}^2 + f_{1cj}^2 + f_{2sj}^2 + f_{2cj}^2 + f_{3sj}^2 + f_{3cj}^2\right) \quad (51)$$

is the average intensity of the jth harmonic of the scattered field. This results directly from the integral $\int_0^{2\pi} \bar{E}_j^2 d(j\eta)$, taking into account Eqs. (46)–(48)

The periodicity property, which has been proved above, is important because it makes it possible to express physical quantities as composite functions of one variable that assume the form $f(\eta) = f(f_1(f_2(f_3(\ldots f_n(\eta)))))$. This strongly simplifies the calculation because, in this case, it is not necessary to write explicitly $f(\eta)$ since its calculation reduces simply to successive calculations of functions f_n, f_3, ..., f_2, f_1, and f, operations that can be performed numerically very fast and accurately [40].

In our case, the quantities $\overline{E}$ and I are composite functions of f_1, f_2, f_3, g_1, g_2, g_3, and γ, which in their turn are periodic functions of η. It follows that the above quantities $\underline{I}_{\rm av}$ and $\underline{I}_j$, which characterize the relativistic Thomson scattering, can be calculated directly with basic mathematics software.

The results presented in this paper were obtained using MATHEMATICA 7, a commercial mathematics computer program. The numerical algorithm implemented in MATHEMATICA 7 comprises two steps: In the first step, we introduce the initial data of the system, which are a_1, a_2, β_{xi}, β_{yi}, β_{zi}, η_i, θ, ϕ, and j. In the second step, we calculate the composite functions in the following order: f_0, f_1, f_2, γ, f_3, g_1, g_2, g_3, F_1, F_2, h_1, h_2, h_3, f_{1c0}, f_{1sj}, f_{1cj}, f_{2c0}, f_{2sj}, f_{2cj}, f_{3c0}, f_{3sj}, f_{3cj}, $\underline{I}_{\rm av}$, and $\underline{I}_j$. The relative errors of our calculations are of the order 10^{-12}. Since the quantities β_{xi}, β_{yi}, β_{zi}, η_i, θ, ϕ, and j enter as arbitrary parameters in the program, any type of variation of the quantities $\underline{I}_{\rm av}$ and $\underline{I}_j$, when these parameters are changed, can be accurately calculated. See Supplemental Material [41] that presents the MATHEMATICA 7 scripts for our calculations.

D. Justification of the classical treatment

In the following analysis, we calculate the divergence of the energy-momentum four-vector, that is, $(p_x, p_y, p_z, H/c)$, where p_x, p_y, p_z are the components of $\overline{p}$, the electron momentum, and H is the total energy. The divergence of this four-vector is [31,36]

$$D = \overline{\nabla}\cdot\overline{p} + \frac{1}{c}\frac{\partial(H/c)}{\partial t} = \frac{\partial}{\partial x}(mc\gamma\beta_x) + \frac{\partial}{\partial y}(mc\gamma\beta_y) + \frac{\partial}{\partial z}(mc\gamma\beta_z) + \frac{1}{c}\frac{\partial}{\partial t}(mc\gamma). \quad (52)$$

We introduce in the above relation the quantities β_x, β_y, γ, and β_z, taken, respectively, from (20), (22), (24), and (25). Taking into account that these quantities are functions of only the phase η, we obtain

$$D = mc\frac{df_1}{d\eta}\frac{\partial\eta}{\partial x} + mc\frac{df_2}{d\eta}\frac{\partial\eta}{\partial y} + mc\frac{df_3}{d\eta}\frac{\partial\eta}{\partial z} + m\frac{d\gamma}{d\eta}\frac{\partial\eta}{\partial t} = -mc\frac{df_3}{d\eta}k_L + m\frac{d\gamma}{d\eta}\omega_L. \quad (53)$$

From (2) and (26), we have, respectively, $c|k_L| = \omega_L$ and $df_3/d\eta = d\gamma/d\eta$ and (53) becomes

$$D = m\frac{d\gamma}{d\eta}(-c|k_L| + \omega_L) = 0. \quad (54)$$

On the other hand, since $\overline{\nabla}S = \overline{p} - e\overline{A}$ and $H = -\partial S/\partial t$ [31,36], where S is the action of the system electron-electromagnetic field and $\overline{A}$ is the magnetic vector potential of the field, the expression of D can be put in the following form:

$$D = \overline{\nabla}\cdot(\overline{\nabla}S + e\overline{A}) + \frac{1}{c}\frac{\partial}{\partial t}\left(\frac{-\partial S}{c\partial t}\right) = \overline{\nabla}\cdot(\overline{\nabla}S + e\overline{A}) - \frac{\partial^2 S}{c^2\partial t^2} = 0. \quad (55)$$

Motz and Selzer [35] proved that, for systems for which the divergence of the energy-momentum four-vector is zero, the Klein-Gordon equation is verified exactly by the classical wave function of the system, that is, $\exp(iS/\hbar)$, where $\hbar$ is the normalized Planck constant. The demonstration of Motz and Selzer is performed without using the WKB approximation. In the Appendix, we present a different demonstration of this property. From this property, it follows that a classical treatment of the system in discussion is justified.

E. Typical calculations of angular and spectral distributions of the scattered beam, compared with theoretical and experimental data from literature

We present a first verification of our calculation method in the particular case when the initial velocity of the electron is neglected. The variation of the normalized intensity $\underline{I}_{\rm av}$ as a function of θ for the case when the laser field is linearly polarized, $a_2 = 0$, $\phi = 0$, $\overline{\beta}_i = 0$, and $\eta_i = 0$, for three values of parameter a_1, is represented in Fig. 1. Our calculation is made for the same initial data as those from Fig. 2(A) of Ref. [42]. Despite the fact that in Ref. [42] the calculation is made with the aid of Eq. (14.67) from Ref. [31], and our calculation was made by the method which has been previously described, the results of the two calculations are almost identical. It is remarkable to see that fine details, such as the small valleys before the maximum of the curves, appear in both calculations. Also, in both cases, the spatial distribution is broad and becomes more collimated as a_1 increases.

Without giving details, we report that our calculations lead to results almost identical to those presented in Fig. 3 from Ref. [42]. These calculations show the influence of the longitudinal component of the electron initial velocity on the angular distribution of the radiation.

Figure 2 shows typical graphs of the normalized averaged intensity $\underline{I}_{\rm av}$ and normalized intensities of the first harmonics

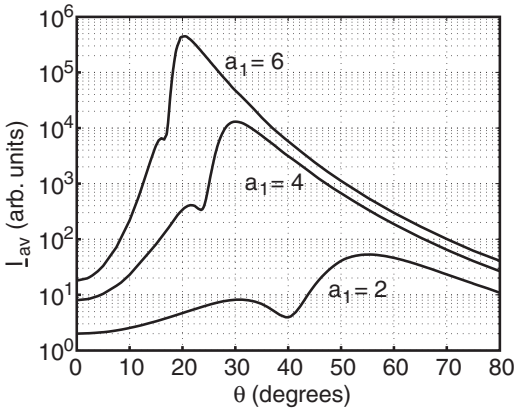

FIG. 1. The variation of the normalized averaged intensity $\underline{I}_{\rm av}$ with θ when the incident field is linearly polarized, $a_2 = 0$, $\phi = 0$, $\overline{\beta}_i = 0$, and $\eta_i = 0$ for three values of parameter a_1.

$\underline{I}_1$ and $\underline{I}_2$ corresponding to $j = 1$ and 2, with respect to θ, for an arbitrary set of values of $a_1, a_2, \beta_{xi}, \beta_{yi}, \beta_{zi}$, and η_i. Since the curves for $j \geqslant 3$ agglomerate below the curve corresponding to $j = 2$, for clarity of the image, we represent only the curves for $j = 1$ and 2. Figure 2 shows that the angular distribution of the global intensity of the scattered radiation is almost identical to the angular distribution of a given harmonic. This result shows that, generally, Eq. (43) can be used for the calculation of the angular distribution of the scattered radiation, while Eq. (51) gives the spectral distribution of the radiation emitted in a given direction.

As it is shown in Ref. [30], a unique analytical result is due to Goreslavskii *et al.* [13] who have obtained, by direct analytical calculation, a closed-form expression for the photon angular distribution corresponding to any initial configuration of the electron and laser beams. Reference [13] shows that, depending on the initial components of the electron velocity, the two emission lobes could became asymmetrical and, in some circumstances, one lobe could be strongly diminished. Our calculations confirm these results, despite the fact that our results are slightly different, as we will show below.

In this respect, we illustrate in Fig. 3 the angular distributions of $\underline{I}_{\rm av}$, normalized to the maximum values, versus

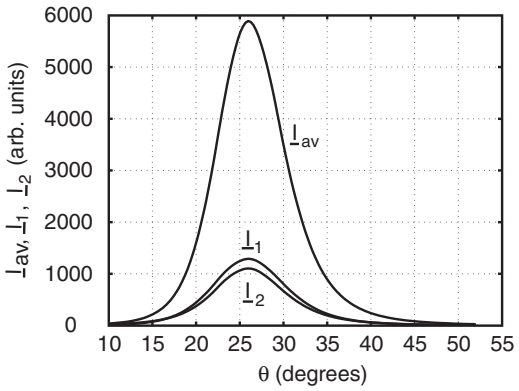

FIG. 2. Typical variations of the normalized averaged intensity $\underline{I}_{\rm av}$ and normalized intensities of the first harmonics $\underline{I}_1$ and $\underline{I}_2$, with θ for $\phi = 0$, $a_1 = 2$, $a_2 = 1.5$, $\beta_{xi} = 0.2$, $\beta_{yi} = 0.2$, $\beta_{zi} = 0.2$, and $\eta_i = 45^\circ$.

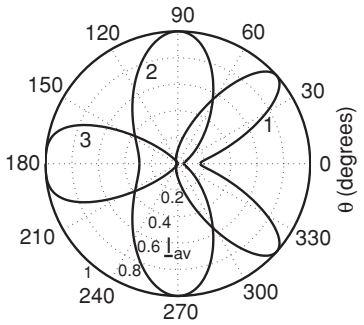

FIG. 3. Polar plots of $\underline{I}_{\rm av}$, normalized to maximum values, as functions of θ in the case of the interaction between a circular polarized field, having $a_1 = a_2 = 2$, which propagate in the oz direction, and relativistic electrons, which move in the opposite direction. Calculations are made for $\phi = 0, \beta_{xi} = \beta_{yi} = 0$, and $\eta_i = 0$ for three cases when $\gamma_i = 1$ and $\beta_{zi} = 0$ (curve 1), $\gamma_i = 1.189$ and $\beta_{zi} = -0.5410$ (curve 2), and $\gamma_i = 3$ and $\beta_{zi} = -0.9428$ (curve 3).

θ in the plane xz in the case of the interaction between a circular polarized field, having $a_1 = a_2 = 2$, which propagate in the oz direction, and relativistic electrons which move in the opposite direction. Calculations are made for $\phi = 0$ and $\eta_i = 0$ for three cases represented by the curves 1, 2, and 3, which correspond, respectively, to $\gamma_i = 1$, $\gamma_i = 1.189$, and $\gamma_i = 3$. These values correspond to $\beta_{zi} = 0$, $\beta_{zi} = -0.5410$, and $\beta_{zi} = -0.9428$, while $\beta_{xi} = \beta_{yi} = 0$ for all three curves. Figure 4 shows the angular distributions $\underline{I}_{\rm av}$, normalized to maximum values, versus θ in the plane xz for $a_1 = a_2 = 2$ when the electron moves in the direction ox, perpendicular to the direction of the incident wave propagation. Calculations are made for $\phi = 0$ and $\eta_i = 0$ for three different initial velocities of the electron represented by the curves 1, 2, and 3. The initial conditions are, respectively, $\gamma_i = 1$, $\gamma_i = 1.1$, and $\gamma_i = 10$, which correspond to $\beta_{xi} = 0$, $\beta_{xi} = 0.4166$, and $\beta_{xi} = 0.9950$, while $\beta_{yi} = \beta_{zi} = 0$ for all three curves.

A comparison between Fig. 3 and Fig. 1 of Ref. [13] reveals that the general properties of the scattered beam are the same

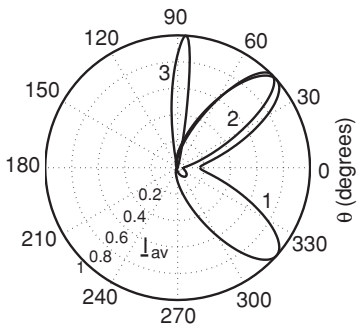

FIG. 4. Polar plots of $\underline{I}_{\rm av}$, normalized to maximum values, as functions of θ in the case of the interaction between a circular polarized field, having $a_1 = a_2 = 2$, which propagate in the oz direction, and relativistic electrons, which move in the ox direction. Calculations are made for $\phi = 0$, $\beta_{yi} = \beta_{zi} = 0$, $\eta_i = 0$ for three cases when $\gamma_i = 1$ and $\beta_{xi} = 0$ (curve 1), $\gamma_i = 1.1$ and $\beta_{xi} = 0.4166$ (curve 2), and $\gamma_i = 10$ and $\beta_{xi} = 0.9950$ (curve 3).

in both cases. The scattering emission lobes are symmetrical and, when the initial electron velocity is small, the radiation is emitted in the oz direction. When the velocity increases, the angle θ_0 between the axis of the emission lobe and the oz axis increases. When the initial electron velocity is sufficiently big, this electron emits radiation in the forward direction with respect to the direction of the initial velocity and in the backward direction with respect to the propagation direction of the incident wave. For very high values of $|\beta_{zi}|$, there is only one backscattered emission lobe. However, there is a difference between our results and those of Ref. [13]. Thus, compared to Fig. 1 of Ref. [13], our Fig. 3 shows an increased component of the backscattered radiation in the negative direction of the oz axis when $|\beta_{zi}|$ is increased.

Figure 4 shows the normalized averaged intensity of the scattered radiation when the electron moves in the direction perpendicular to the direction of the incident wave propagation. Different initial velocities of the electron are considered. A comparison between this figure and Fig. 2 of Ref. [13] shows similar properties of the scattered beam. More specifically, when $|\beta_{xi}|$ increases, the emission lobes are asymmetrical, one lobe is diminished, and the bigger emission lobe is shifted toward the ox direction. However, unlike Fig. 2 of Ref. [13], we obtained that, for sufficiently high values of the initial electron velocity corresponding to $\gamma_i > 4$, one emission lobe is completely diminished.

In spite of the fact that, for some directions of the initial velocity of the electron, the emission lobes become asymmetrical, the shape of the scattered radiation spectrum remains the same for relatively high values of a_1 and a_2. Figure 5 shows such a spectrum, namely, the variation of $\underline{I}_j$ with j when the incident electromagnetic field is elliptically polarized. For this example, we chose the values of θ and ϕ that correspond to the maximum value of $\underline{I}_{\rm av}$, namely, to the top of the lobe, and the values of a_1, a_2, β_{xi}, β_{yi}, β_{zi}, and η_i given in the caption of Fig. 5. Similar figures can be derived for other values of these parameters. The spectrum of Fig. 5 has an increasing portion for small values of j, a maximum and a slow decreasing portion for high values of j, its shape being similar to the spectrum shown in Fig. 7 of Ref. [42].

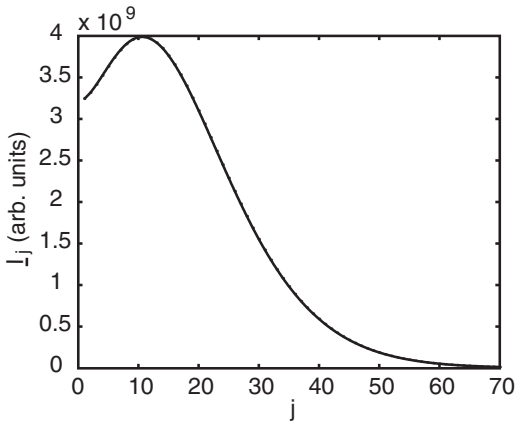

FIG. 5. Typical spectral distribution of the scattered Thomson radiation, namely, the variation of $\underline{I}_j$ with j, when the incident electromagnetic field is elliptically polarized for $\theta = 4.182^\circ$, $\phi = -15.1^\circ$, $a_1 = 15$, $a_2 = 10$, $\beta_{xi} = 0.15$, $\beta_{yi} = -0.10$, $\beta_{zi} = 0.20$, and $\eta_i = 30^\circ$.

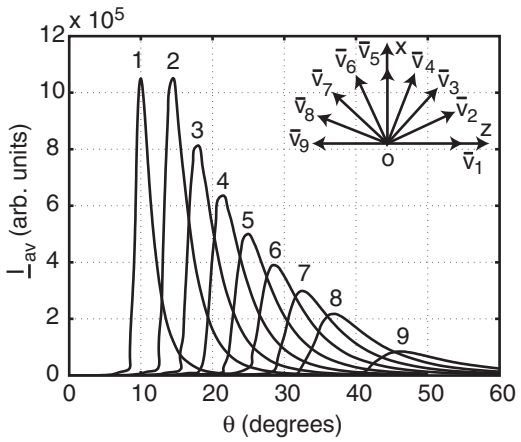

FIG. 6. Typical angular distributions of $\underline{I}_{\rm av}$ versus θ when the laser field interacts with nine electrons, the velocities of which are situated in the the plane xz, as shown in the inset, for $a_1 = 5.6$, $a_2 = 0$, $\phi = 0$, and $\eta_i = 0$. Curve 1 corresponds to the electron having the initial velocity $\overline{\beta}_i = \overline{v}_1/c$, and so on. The initial velocities are as follows: $\beta_{xi} = 0$, $\beta_{yi} = 0$, $\beta_{zi} = 0.6574$ for curve 1, $\beta_{xi} = 0.4792$, $\beta_{yi} = 0$, $\beta_{zi} = 0.45$ for curve 2, $\beta_{xi} = 0.5850$, $\beta_{yi} = 0$, $\beta_{zi} = 0.30$ for curve 3, $\beta_{xi} = 0.6401$, $\beta_{yi} = 0$, $\beta_{zi} = 0.15$ for curve 4, $\beta_{xi} = 0.6574$, $\beta_{yi} = 0$, $\beta_{zi} = 0$ for curve 5, $\beta_{xi} = 0.6401$, $\beta_{yi} = 0$, $\beta_{zi} = 0 - 0.15$ for curve 6, $\beta_{xi} = 0.5850$, $\beta_{yi} = 0$, $\beta_{zi} = -0.30$ for curve 7, $\beta_{xi} = 0.4792$, $\beta_{yi} = 0$, $\beta_{zi} = -0.45$ for curve 8, and $\beta_{xi} = 0$, $\beta_{yi} = 0$, $\beta_{zi} = -0.6574$ for curve 9.

Now we show that the angular distributions of $\underline{I}_{\rm av}$ when the laser field interact with electrons having nonzero initial velocities is broader than the theoretical prediction when the initial electron is at rest, in agreement with experimental data from literature. Assume that the average initial total energy of the electrons, denoted by E_i, is equal to 0.9 MeV, which corresponds, by virtue of the relation $E_i = mc^2/\sqrt{1-\overline{\beta}_i{}^2}$, to the value $|\overline{\beta}_i| = 0.6574$. Figure 6 shows typical variations of $\underline{I}_{\rm av}$ with θ, for $a_1 = 5.6$, $a_2 = 0$, $\phi = 0$, and $\eta_i = 0$ when the laser field interacts with many electrons (particularly, we consider nine electrons), with the directions of the initial velocities of the electrons, denoted by $\overline{v}_1, \overline{v}_2, \ldots, \overline{v}_9$, being uniformly distributed in the plane xz, as illustrated in the inset. Figure 7 shows similar variations of $\underline{I}_{\rm av}$ with θ, for $a_1 = 5.6$, $a_2 = 0$, $\phi = 0$, and $\eta_i = 0$, when the directions of the initial velocities of five electrons, denoted by $\overline{v}_1, \overline{v}_2, \ldots, \overline{v}_5$, are uniformly distributed in the plane xy, as it is shown in the inset. The analysis of Fig. 6 shows that the global angular distribution of $\underline{I}_{\rm av}$ with respect to θ is comprised between the curves that correspond to the forward and backward directions of the initial electron velocities with respect to the oz axis, namely, in our case, by the curves 1 and 9. We notice that the angular distribution of the Thomson scattered radiation is significantly broadened to approximately 40°, compared to the theoretical width of around 15° if the electron is initially at rest, as it results from Fig. 1. This broadening is similar to that from Fig. 6 of Ref. [42], which represents the spatial distribution of the observed scattered Thomson radiation when the initial electron energies are around 0.9 MeV. On the other hand, Fig. 7 shows that electron 3, the initial velocity of which

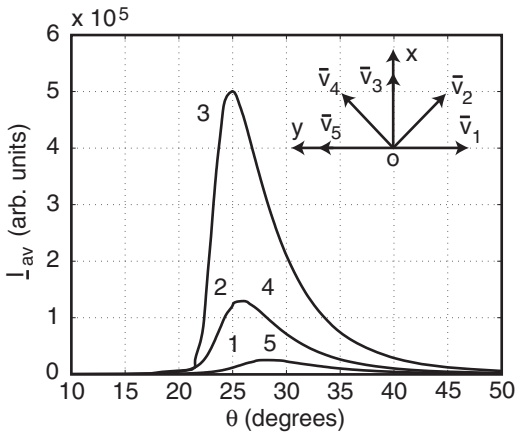

FIG. 7. Typical angular distributions of $\underline{I}_{\rm av}$ versus θ when the laser field interacts with five electrons, the velocities of which are situated in the the plane xy, as it is shown in the inset, for $a_1 = 5.6$, $a_2 = 0, \phi = 0$, and $\eta_i = 0$. Curve 1 corresponds to the electron having the initial velocity $\overline{\beta}_i = \overline{v}_1/c$, and so on. The initial velocities are as follows: $\beta_{xi} = 0, \beta_{yi} = -0.6574, \beta_{zi} = 0$ for curve 1, $\beta_{xi} = 0.4649$, $\beta_{yi} = -0.4649, \beta_{zi} = 0$ for curve 2, $\beta_{xi} = 0.6574, \beta_{yi} = 0, \beta_{zi} = 0$ for curve 3, $\beta_{xi} = 0.4649, \beta_{yi} = 0.4649, \beta_{zi} = 0$ for curve 4, and $\beta_{xi} = 0, \beta_{yi} = 0.6574, \beta_{zi} = 0$ for curve 5. The curve 1 is identical to the curve 5, while the curve 2 is identical to the curve 4.

is directed toward the ox axis, has a dominant contribution to the global scattered spectrum. Thus, the electrons situated in the xz plane have also a dominant contribution. This is an explanation of the fact that the shape of the envelope of the curves in Fig. 6 is very similar to the shape of the curve from Fig. 6 of Ref. [42].

III. COMPOSITE FUNCTIONS IN THE CASE OF HARD BACKSCATTERED RADIATIONS GENERATED BY INTERACTION BETWEEN RELATIVISTIC ELECTRONS AND VERY INTENSE ELECTROMAGNETIC BEAMS

A. Analysis of the electron motion in the system of reference in which the initial electron velocity is zero

The generation of backscattered radiation when the electromagnetic beam and relativistic electrons collide head-on with each other is a very promising souce of hard x rays [17–24]. In this case, the initial data from Sec. II A remain valid, with the difference that the initial conditions, written in the laboratory reference system, denoted by $S(t,x,y,z)$, are as follows:

$$t = 0,\ \ x = y = z = 0,\ \ v_x = v_y = 0,$$
$$v_z = -|V_0|, \quad \text{and} \quad \eta = \eta_i. \tag{56}$$

By virtue of the theory presented in Sec. 5.22 of Ref. [43], it is convenient to calculate the motion of the electron in the inertial system of reference denoted by $S'(t',x',y',z')$, in which the initial velocity of the electron is zero. The Cartesian axes in the systems $S(t,x,y,z)$ and $S'(t',x',y',z')$ are parallel. In our case, the S' system moves with velocity $-|V_0|$ along the oz axis (Fig. 8). Since our analysis is performed in the S' system, we have to calculate the parameters of the laser field, denoted by $\overline{E}'_L$, $\overline{B}'_L$, $\overline{k}'_L$, and ω'_L, in the S' system.

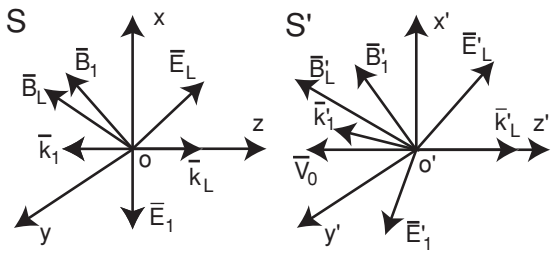

FIG. 8. Components of the laser field and of the field generated by Thomson scattering in the S and S' systems.

The four-dimensional wave vectors are denoted, respectively, by $(\frac{\omega_L}{c}, k_{Lx}, k_{Ly}, k_{Lz})$ and $(\frac{\omega'_L}{c}, k'_{Lx'}, k'_{Ly'}, k'_{Lz'})$ in the systems S and S'. By virtue of the Lorentz transformation, given by relations (11.22) of Ref. [31], we have

$$\frac{\omega'_L}{c} = \frac{\omega_L}{c}\gamma_0(1 + |\beta_0|), \tag{57}$$
$$k'_{Lz'} = |k'_L| = |k_L|\gamma_0(1 + |\beta_0|), \tag{58}$$
$$k'_{Lx'} = k_{Lx} = k'_{Ly'} = k_{Ly} = 0, \tag{59}$$

where

$$\overline{\beta}_0 = -\frac{|V_0|}{c}\overline{k} \quad \text{and} \quad \gamma_0 = \left(1 - \beta_0^2\right)^{-\frac{1}{2}}. \tag{60}$$

Since the scalar product between the four-dimensional wave vector and the space-time four-vector is invariant, it follows that the phase of the electromagnetic wave is invariant [31], and we have

$$\eta = \omega_L t - \overline{k}_L \cdot \overline{r} + \eta_i = \omega'_L t' - \overline{k}'_L \cdot \overline{r}' + \eta_i = \eta', \tag{61}$$

where $\overline{r}$ and $\overline{r}'$ are the position vectors of the electron in the two systems.

We use Eqs. (11.149) from Ref. [31], which give the Lorentz transformation of the fields. By writing these relations in the International System, and using Eqs. (4) and (60), we obtain the following expressions for the components of the electromagnetic field in the S' system:

$$\overline{E}'_L = \gamma_0(\overline{E}_L + \overline{\beta}_0 \times c\overline{B}_L) = \gamma_0(1 + |\beta_0|)\overline{E}_L, \tag{62}$$
$$\overline{B}'_L = \gamma_0(\overline{B}_L - \overline{\beta}_0 \times \overline{E}_L/c) = \gamma_0(1 + |\beta_0|)\overline{B}_L. \tag{63}$$

The equations of motion of the electron in the S' system can be written as

$$m\frac{d}{dt'}(\gamma' v'_{x'}) = \gamma_0(1 + |\beta_0|)(-eE_{M1}\cos\eta' + ev'_{z'}B_{M1}\cos\eta'), \tag{64}$$
$$m\frac{d}{dt'}(\gamma' v'_{y'}) = \gamma_0(1 + |\beta_0|)(-eE_{M2}\sin\eta' + ev'_{z'}B_{M2}\sin\eta'), \tag{65}$$
$$m\frac{d}{dt'}(\gamma' v'_{z'}) = \gamma_0(1 + |\beta_0|)(-ev'_{x'}B_{M1}\cos\eta' - ev'_{y'}B_{M2}\sin\eta'), \tag{66}$$

where $v'_{x'}$, $v'_{y'}$, and $v'_{z'}$ are the components of the electron velocity in S' and

$$\gamma' = \left(1 - {\beta'_{x'}}^2 - {\beta'_{y'}}^2 - {\beta'_{z'}}^2\right)^{-\frac{1}{2}} \tag{67}$$

with $\beta'_{x'} = v'_{x'}/c$, $\beta'_{y'} = v'_{y'}/c$, and $\beta'_{z'} = v'_{z'}/c$.

By using Eqs. (4) and (57), the equations of motion become

$$\frac{d}{dt'}(\gamma'\beta'_{x'}) = -a'_1\omega'_L(1-\beta'_{z'})\cos\eta', \tag{68}$$

$$\frac{d}{dt'}(\gamma'\beta'_{y'}) = -a'_2\omega'_L(1-\beta'_{z'})\sin\eta', \tag{69}$$

$$\frac{d}{dt'}(\gamma'\beta'_{z'}) = -\omega'_L(a'_1\beta'_{x'}\cos\eta' + a'_2\beta'_{y'}\sin\eta'), \tag{70}$$

where

$$a'_1 = \frac{\gamma_0(1+|\beta_0|)eE_{M1}}{mc\omega'_L} = a_1 \quad \text{and}$$

$$a'_2 = \frac{\gamma_0(1+|\beta_0|)eE_{M2}}{mc\omega'_L} = a_2. \tag{71}$$

Remarkably, the relativistic constants a_1 and a_2 are invariants and Eqs. (68)–(70) have the same form as (12)–(14). Since the analysis is made in the system S', the only difference is with respect to the initial conditions, which are

$$t' = 0,\ x' = y' = z' = 0,\ v'_{x'} = 0,\ v'_{y'} = 0,$$
$$v'_{z'} = 0, \quad \text{and} \quad \eta = \eta' = \eta_i. \tag{72}$$

An identical procedure as that of Sec. II B leads to the following solution of the equation system (68)–(70):

$$f'_1 = f'_1(\eta') = -a_1(\sin\eta' - \sin\eta_i), \tag{73}$$

$$f'_2 = f'_2(\eta') = -a_2(\cos\eta_i - \cos\eta'), \tag{74}$$

$$\gamma' = \gamma'(\eta') = \frac{1}{2}\left(2 + {f'_1}^2 + {f'_2}^2\right), \tag{75}$$

$$f'_3 = f'_3(\eta') = \gamma' - 1, \tag{76}$$

$$\beta'_{x'} = \frac{f'_1}{\gamma'}, \tag{77}$$

$$\beta'_{y'} = \frac{f'_2}{\gamma'}, \tag{78}$$

$$\beta'_{z'} = \frac{f'_3}{\gamma'}, \tag{79}$$

$$g'_1 = g'_1(\eta') = -\frac{a_1}{\gamma'^2}\cos\eta' + \frac{f'_1}{\gamma'^3}(a_1 f'_1\cos\eta' + a_2 f'_2\sin\eta'), \tag{80}$$

$$g'_2 = g'_2(\eta') = -\frac{a_2}{\gamma'^2}\sin\eta' + \frac{f'_2}{\gamma'^3}(a_1 f'_1\cos\eta' + a_2 f'_2\sin\eta'), \tag{81}$$

$$g'_3 = g'_3(\eta') = -\frac{1}{\gamma'^3}(a_1 f'_1\cos\eta' + a_2 f'_2\sin\eta'), \tag{82}$$

$$\dot\beta'_{x'} = \omega'_L g'_1, \tag{83}$$

$$\dot\beta'_{y'} = \omega'_L g'_2, \tag{84}$$

$$\dot\beta'_{z'} = \omega'_L g'_3. \tag{85}$$

From these relations, we observe that the functions f'_1, f'_2, γ', f'_3, g'_1, g'_2, g'_3, $\beta'_{x'}$, $\beta'_{y'}$, $\beta'_{z'}$, $\dot\beta'_{x'}$, $\dot\beta'_{y'}$, and $\dot\beta'_{z'}$ are periodic functions of one variable η'.

B. Periodicity of the electromagnetic field in the S' system

The periodicity of the scattered electromagnetic field results directly from the Lièнard-Wiechert relation, by virtue of the periodicity of $\bar\beta'$ and $\dot{\bar\beta}'$. In the S' system, the Liènard-Wiechert relation is

$$\overline{E}' = \frac{-e}{4\pi\varepsilon_0 cR'}\frac{\overline{n}'\times[(\overline{n}'-\overline{\beta}')\times\dot{\overline{\beta}}']}{(1-\overline{n}'\cdot\overline{\beta}')^3}, \tag{86}$$

where R' is the distance from the electron to the observation point (the detector) and $\overline{n}'$ is the versor of the direction electron detector. We calculate the right-hand side of Eq. (86) at time t'. By virtue of the significance of the quantities entering in the Liènard-Wiechert equation, it results that the field $\overline{E}'$ corresponds to the time $t' + R'/c$ and we have $\overline{E}' = \overline{E}'(\overline{r}' + \overline{R}', t' + R'/c)$, where $\overline{R}' = R'\overline{n}'$. The inequality $R' \gg r'$ is strongly fulfilled. In the S' system, the expression of the versor $\overline{n}'$ is

$$\overline{n}' = \overline{i}\sin\theta'\cos\phi' + \overline{j}\sin\theta'\sin\phi' + \overline{k}\cos\theta', \tag{87}$$

where θ' is the azimuthal angle between the $\overline{n}'$ and $\overline{k}$ versors and ϕ' is the polar angle in the plane $x'y'$.

Introducing the components of $\overline{n}'$, $\bar\beta'$, and $\dot{\bar\beta}'$ from the above relations in (86), we obtain the following expression of the intensity of the scattered electric field in system S':

$$\overline{E}' = \frac{K'}{{F'_1}^3}\left(h'_1\overline{i} + h'_2\overline{j} + h'_3\overline{k}\right) \quad \text{with} \quad K' = \frac{-e\omega'_L}{4\pi\varepsilon_0 cR'}, \tag{88}$$

where

$$h'_1 = F'_2\left(n'_{x'} - \frac{f'_1}{\gamma'}\right) - F'_1 g'_1, \tag{89}$$

$$h'_2 = F'_2\left(n'_{y'} - \frac{f'_2}{\gamma'}\right) - F'_1 g'_2, \tag{90}$$

$$h'_3 = F'_2\left(n'_{z'} - \frac{f'_3}{\gamma'}\right) - F'_1 g'_3 \tag{91}$$

with

$$F'_1 = 1 - n'_{x'}\frac{f'_1}{\gamma'} - n'_{y'}\frac{f'_2}{\gamma'} - n'_{z'}\frac{f'_3}{\gamma'}, \tag{92}$$

$$F'_2 = n'_{x'}g'_1 + n'_{y'}g'_2 + n'_{z'}g'_3, \tag{93}$$

$$n'_{x'} = \sin\theta'\cos\phi', \quad n'_{y'} = \sin\theta'\sin\phi', \quad \text{and}$$
$$n'_{z'} = \cos\theta'. \tag{94}$$

Since the components of the field given by (88) are periodic functions of η', they can be developed in Fourier series and the

expression of the field normalized to K' becomes

$$\frac{\bar{E}'}{K'} = f'_{1c0}\bar{i} + \left(\sum_{j=1}^{\infty} f'_{1sj}\sin j\eta' + \sum_{j=1}^{\infty} f'_{1cj}\cos j\eta'\right)\bar{i} + f'_{2c0}\bar{j} + \left(\sum_{j=1}^{\infty} f'_{2sj}\sin j\eta' + \sum_{j=1}^{\infty} f'_{2cj}\cos j\eta'\right)\bar{j} + f'_{3c0}\bar{k} + \left(\sum_{j=1}^{\infty} f'_{3sj}\sin j\eta' + \sum_{j=1}^{\infty} f'_{3cj}\cos j\eta'\right)\bar{k}, \tag{95}$$

where

$$f'_{\alpha c0} = \frac{1}{2\pi}\int_0^{2\pi} \frac{h'_\alpha}{F_1'^3} d\eta'; \quad f'_{\alpha sj} = \frac{1}{\pi}\int_0^{2\pi} \frac{h'_\alpha}{F_1'^3}\sin j\eta' d\eta';$$
$$f'_{\alpha cj} = \frac{1}{\pi}\int_0^{2\pi} \frac{h'_\alpha}{F_1'^3}\cos j\eta' d\eta' \tag{96}$$

with $\alpha = 1,2,3$.

The quantity

$$\bar{E}'_j = \bar{E}'_{js} + \bar{E}'_{jc}, \tag{97}$$

where

$$\bar{E}'_{js} = K'\left(f'_{1sj}\bar{i} + f'_{2sj}\bar{j} + f'_{3sj}\bar{k}\right)\sin j\eta' = K'\left(f'_{1sj}\bar{i} + f'_{2sj}\bar{j} + f'_{3sj}\bar{k}\right)\cos j(\eta' - \pi/2) \tag{98}$$

and

$$\bar{E}'_{jc} = K'\left(f'_{1cj}\bar{i} + f'_{2cj}\bar{j} + f'_{3cj}\bar{k}\right)\cos j\eta' \tag{99}$$

is the intensity of the jth harmonic of the electric field. This harmonic is obtained by the addition of two plane electromagnetic fields, the intensities of which are, respectively, $\bar{E}'_{js}$ and $\bar{E}'_{jc}$. These fields have phases $j(\eta' - \pi/2)$ and $j\eta'$ and the same angular frequency and absolute value of the wave vector, which are equal to $j\omega'_L$ and $j|\bar{k}'_L| = j\omega'_L/c$, respectively.

The corresponding components of the magnetic field are

$$\bar{B}'_{js} = \bar{n}' \times \frac{\bar{E}'_{js}}{c} \quad \text{and} \quad \bar{B}'_{jc} = \bar{n}' \times \frac{\bar{E}'_{jc}}{c}. \tag{100}$$

In the same time, $\bar{E}'_j$ is a function of θ' and ϕ', consequently, it is easy to calculate the spectral structure of the field emitted in a given direction specified by the versor $\bar{n}'$ as follows. By virtue of relations (57) and (58), the angular frequency and wave vector, corresponding to this direction, are given by the following relations:

$$\omega'_j = j\omega'_L = j\omega_L\gamma_0(1 + |\beta_0|), \tag{101}$$
$$\bar{k}'_j = j|\bar{k}'_L|\bar{n}' = j|k_L|\gamma_0(1 + |\beta_0|)\bar{n}'. \tag{102}$$

The fundamental component of the frequency corresponds to $j = 1$. Since the experimental data regarding hard-x-ray generation presently available for the interaction between relativistic electrons and very intense laser beams corresponds to the case when the fundamental component is dominant [17,18], we limit our analysis to this case. From the theory presented above, it follows that harmonics of this frequency is possible. Recently, this result was proved experimentally [34].

C. Relations between azimuthal and polar angles in the S and S' systems

By virtue of Eqs. (101) and (102), the angular frequency and the wave vector corresponding to the fundamental scattered radiation (i.e., $j = 1$) for an arbitrary direction specified by θ' and ϕ' in the S' system are given by the relations

$$\omega'_1 = \omega'_L = \omega_L\gamma_0(1 + |\beta_0|), \tag{103}$$

$$\bar{k}'_1 = |\bar{k}'_1|\bar{n}' = |\bar{k}'_1|\bar{i}\sin\theta'\cos\phi' + |\bar{k}'_1|\bar{j}\sin\theta'\sin\phi' + |\bar{k}'_1|\bar{k}\cos\theta', \tag{104}$$

where

$$|\bar{k}'_1| = |k_L|\gamma_0(1 + |\beta_0|) = \omega'_1/c. \tag{105}$$

We use again the Lorentz relations to calculate the angular frequency and the wave vector for the fundamental radiation, denoted, respectively, by ω_1 and $\bar{k}_1$, in the laboratory system S. As before, we apply relations (11.22) from Ref. [31], taking into account (60) and (103)–(105), and find ω_1 and the components of $\bar{k}_1$, as follows:

$$\frac{\omega_1}{c} = \gamma_0\left(\frac{\omega'_1}{c} + \bar{\beta}_0\cdot\bar{k}'_1\right) = \gamma_0|\bar{k}'_1|(1 - |\beta_0|\cos\theta'), \tag{106}$$

$$k_{1z} = \gamma_0\left(k'_{1z'} - |\beta_0|\frac{\omega'_1}{c}\right) = \gamma_0|\bar{k}'_1|(\cos\theta' - |\beta_0|), \tag{107}$$

$$k_{1x} = k'_{1x'} = |\bar{k}'_1|\sin\theta'\cos\phi', \tag{108}$$

$$k_{1y} = k'_{1y'} = |\bar{k}'_1|\sin\theta'\sin\phi'. \tag{109}$$

From (106)–(110), it is easy to verify that

$$|\bar{k}_1| = \frac{\omega_1}{c}. \tag{110}$$

On the other hand, from (107), we have $k_{1z} = |\bar{k}_1|\cos\theta = \gamma_0|\bar{k}'_1|(\cos\theta' - |\beta_0|)$ and from (106) and (110), we obtain

$$\cos\theta = \frac{\cos\theta' - |\beta_0|}{1 - |\beta_0|\cos\theta'}. \tag{111}$$

This equation allows us to calculate the angle θ in the S system, which corresponds to angle θ' in the S' system. We note that this relation is identical to relation (5.6) from Landau's book [36], which has been deduced in a completely different way.

On the other hand, since in the S system the wave propagates in the direction of the versor $\bar{n}$ (the components of which are $\sin\theta\cos\phi$, $\sin\theta\sin\phi$, and $\cos\theta$) and $k_{1x} = |\bar{k}_1|\sin\theta\cos\phi$ and $k_{1y} = |\bar{k}_1|\sin\theta\sin\phi$, it follows from these relations and (108) and (109) that

$$\phi = \phi'. \tag{112}$$

D. Spectral and angular distributions in the laboratory system.

By virtue of Eqs. (58) and (106), we obtain the quanta energy of the fundamental radiations in the system S, denoted by W_1, as a function of θ':

$$W_1 = \omega_1\hbar = \omega_L\gamma_0^2(1 + |\beta_0|)(1 - |\beta_0|\cos\theta')\hbar. \tag{113}$$

The energy of the backscattered radiation corresponds to $\theta' = \theta = \pi$. We note it by W_{b1} and the corresponding frequency by ω_{b1}, and have

$$W_{b1} = \omega_{b1}\hbar = \omega_L \gamma_0^2 (1 + |\beta_0|)^2 \hbar. \tag{114}$$

The corresponding wavelength of the backscattered radiation is

$$\lambda_{b1} = \frac{\lambda_L}{\gamma_0^2 (1 + |\beta_0|)^2}, \tag{115}$$

where λ_L is the wavelength of the incident laser beam.

We use again the Lorentz transformations of the fields given by Eqs. (11.149) from Ref. [31], and calculate the fundamental component $\bar{E}_{1s}$ in the system S. From (98) and (100), we obtain, for $j = 1$,

$$\begin{aligned}\bar{E}_{1s} &= \gamma_0(\bar{E}'_{1s} - \overline{\beta}_0 \times c\bar{B}'_{1s}) - \frac{\gamma_0^2}{\gamma_0 + 1}\overline{\beta}_0(\overline{\beta}_0 \cdot \overline{E}'_{1s}) \\ &= \gamma_0(1 - |\beta_0|\cos\theta')\bar{E}'_{1s} \\ &\quad + K'\gamma_0|\beta_0| f'_{3s1} \sin\eta' \left(\overline{n}' - \frac{\gamma_0|\beta_0|}{\gamma_0 + 1}\overline{k}\right).\end{aligned} \tag{116}$$

Similarly, we have

$$\begin{aligned}\bar{E}_{1c} &= \gamma_0(1 - |\beta_0|\cos\theta')\bar{E}'_{1c} \\ &\quad + K'\gamma_0|\beta_0| f'_{3c1} \cos\eta' \left(\overline{n}' - \frac{\gamma_0|\beta_0|}{\gamma_0 + 1}\overline{k}\right).\end{aligned} \tag{117}$$

From Eqs. (87), (97)–(99), (116), and (117) and taking into account that the phase of the electromagnetic field is a relativistic invariant, namely, $\eta = \eta'$, we obtain the expression for the intensity of the fundamental electrical field in the system S:

$$\bar{E}_1 = \bar{E}_{1s} + \bar{E}_{1c} = E_{1x}\overline{i} + E_{1y}\overline{j} + E_{1z}\overline{k}, \tag{118}$$

where

$$E_{1x} = K' I_{1s1} \sin\eta + K' I_{1c1} \cos\eta, \tag{119}$$

$$E_{1y} = K' I_{2s1} \sin\eta + K' I_{2c1} \cos\eta, \tag{120}$$

$$E_{1z} = K' I_{3s1} \sin\eta + K' I_{3c1} \cos\eta \tag{121}$$

with

$$I_{1s1} = \gamma_0(1 - |\beta_0|\cos\theta') f'_{1s1} + \gamma_0|\beta_0|\sin\theta'\cos\phi' f'_{3s1}, \tag{122}$$

$$I_{1c1} = \gamma_0(1 - |\beta_0|\cos\theta') f'_{1c1} + \gamma_0|\beta_0|\sin\theta'\cos\phi' f'_{3c1}, \tag{123}$$

$$I_{2s1} = \gamma_0(1 - |\beta_0|\cos\theta') f'_{2s1} + \gamma_0|\beta_0|\sin\theta'\sin\phi' f'_{3s1}, \tag{124}$$

$$I_{2c1} = \gamma_0(1 - |\beta_0|\cos\theta') f'_{2c1} + \gamma_0|\beta_0|\sin\theta'\sin\phi' f'_{3c1}, \tag{125}$$

$$I_{3s1} = f'_{3s1}, \tag{126}$$

$$I_{3c1} = f'_{3c1}. \tag{127}$$

The averaged value of the intensity of the fundamental component of the scattered radiation, normalized to $\epsilon_0 c K'^2$, is given by

$$\underline{I}_1 = \frac{I_1}{\epsilon_0 c K'^2} = \frac{1}{2\pi}\int_0^{2\pi} \frac{1}{K'^2}\left(E_{1x}^2 + E_{1y}^2 + E_{1z}^2\right) d\eta. \tag{128}$$

Taking into account (119)–(121) and (128), a simple calculation leads to the relation

$$\underline{I}_1 = \tfrac{1}{2}\left(I_{1s1}^2 + I_{1c1}^2 + I_{2s1}^2 + I_{2c1}^2 + I_{3s1}^2 + I_{3c1}^2\right). \tag{129}$$

The numerical calculation procedure is identical to that which has been described in Sec. II C, with the difference that, in this case, the initial data comprise a_1, a_2, η_i, θ', and ϕ'. Since $\overline{E}_1$ and I_1 are composite functions of η, the calculation of $\underline{I}_1$ reduces to the successive calculations of the following functions: f'_1, f'_2, γ', f'_3, g'_1, g'_2, g'_3, F'_1, F'_2, h'_1, h'_2, h'_3, f'_{1s1}, f'_{1c1}, f'_{2s1}, f'_{2c1}, f'_{3s1}, f'_{3c1}, I_{1s1}, I_{1c1}, I_{2s1}, I_{2c1}, I_{3s1}, I_{3c1}, and $\underline{I}_1$. The calculation of W_1 and $\underline{I}_1$, given, respectively, by (113) and (129), as functions of θ' is made with the aid of MATHEMATICA 7. See Supplemental Material [41] that presents the MATHEMATICA 7 scripts for our calculations.

E. Comparison between theoretical and experimental data

As a practical application, we evaluate now the angular and spectral distribution of the backscattered radiation in two cases wherein a linearly polarized laser beam (for which $E_2 = 0$ and $a_2 = 0$) collides head-on with relativistic electrons. In the first case, the wavelength of the laser beam is $\lambda_L = 10.64$ μm, the pulse duration is $\tau_L = 180 \times 10^{-12}$ s, the radius of the laser beam $r_L = 32$ μm, the energy of the laser pulse is $W_L = 0.2$ J, and the energy of the electrons is $E_i = 60$ MeV. From the relations $\gamma_0 = E_i/(mc^2)$, $I_L = E_i/(\pi r_L^2 \tau_L)$, $E_{M1} = \sqrt{2I_L/(\epsilon_0 c)}$, $\omega_L = 2\pi c/(\lambda_L)$, and $a_1 = eE_{M1}/(mc\omega_L)$, we calculate γ_0, I_L, E_{M1}, ω_L, and a_1, the values of which are given in the caption of Table I. In the second case, we have $\lambda_L = 0.800$ μm, $\tau_L = 54 \times 10^{-15}$ s, $r_L = 35$ μm, $W_L = 0.180$ J, and $E_i = 57$ MeV.

With the aid of Eq. (111), we calculate the values of θ as function of θ', when θ' takes values between $\pi/2$, and π. The last angle corresponds to radiations scattered in the backward direction. With the aid of MATHEMATICA 7 and the procedure described in the preceding section, we calculate the variations of W_1 and $\underline{I}_1$ as functions of θ' and show these values in Table I. In this table, we also show the corresponding values of the angle α given by the relation

$$\alpha = \pi - \theta. \tag{130}$$

Taking into account the values from Table I, in Fig. 9 we record the angular variations of the intensity of the backscattered radiation $\underline{I}_1$ as function of α, and the spectral variations of W_1 as function of α for the two cases described above. These curves are symmetrical with respect to the direction corresponding to $\theta = \pi$.

Cases 1 and 2 correspond, respectively, to the experimental data from Refs. [17] and [18]. The analysis of the curves $\underline{I}_1 = \underline{I}_1(\alpha)$ from Fig. 9 shows that the agreement between the theoretical and experimental values of the divergence angle of the backscattered beam, denoted by $\Delta\alpha$, is very good. From the curve $\underline{I}_1 = \underline{I}_1(\alpha)$ of Fig. 9(a), we obtain $\Delta\alpha = 8$ mrad,

TABLE I. Variations of θ (in rad), $\alpha = \pi - \theta$ (in mrad), $\underline{I}_1$ and W_1 (in keV) with respect to θ' (in degrees) in two cases. In the first case, $E_i = 60$ MeV, $\gamma_0 = 117.4$, $|\beta_0| = 0.999\,96$, $I_L = 3.454 \times 10^{17}$ Wm^{-2}, $E_{M1} = 1.613 \times 10^{10}$ Vm^{-1}, $\omega_L = 1.770 \times 10^{14}$ rad s^{-1}, $\phi' = 0$, $\eta_i = 0$, $a_1 = 0.053\,46$, $a_2 = 0$, and $W_{b1} = 6.42$ keV. In the second case, $E_i = 57$ MeV, $\gamma_0 = 111.5$, $|\beta_0| = 0.999\,96$, $I_L = 8.661 \times 10^{20}$ Wm^{-2}, $E_{M1} = 8.078 \times 10^{11}$ Vm^{-1}, $\omega_L = 2.355 \times 10^{15}$ rad s^{-1}, $\phi' = 0$, η_i=0, $a_1 = 0.2012$, $a_2 = 0$, and $W_{b1} = 77.08$ keV.

Case 1											
θ' (deg)	90	100	110	120	130	140	150	160	170	175	180
θ (rad)	3.1331	3.1345	3.1356	3.1367	3.1376	3.1385	3.1393	3.1401	3.1408	3.1412	3.1416
α (mrad)	8.52	7.15	5.96	4.92	3.97	3.10	2.28	1.51	0.75	0.37	0.00
$\underline{I}_1$	0.0	8.3	41.5	110.2	217.5	355.9	506.5	643.1	783.7	764.3	773.1
W_1 (keV)	3.21	3.77	4.31	4.82	5.28	5.67	5.99	6.23	6.37	6.41	6.42
Case 2											
θ' (deg)	90	100	110	120	130	140	150	160	170	175	180
θ (rad)	3.1326	3.1341	3.1353	3.1364	3.1374	3.1383	3.1392	3.1400	3.1408	3.1412	3.1416
α (mrad)	8.97	7.53	6.28	5.18	4.18	3.26	2.40	1.58	0.78	0.39	0.00
$\underline{I}_1$	1.6	142.7	621.8	1542.9	2900.6	4560.2	6284.5	7790.2	8815.9	9087.6	9179.5
W_1 (keV)	38.54	45.23	51.72	57.81	63.31	68.06	71.92	74.76	76.50	76.93	77.08

which is the same as the value reported in Ref. [17]. Also, the theoretical curve $\underline{I}_1 = \underline{I}_1(\alpha)$ from Fig. 9(b) is almost identical to the experimental curve shown in Fig. 3(b) from Ref. [18].

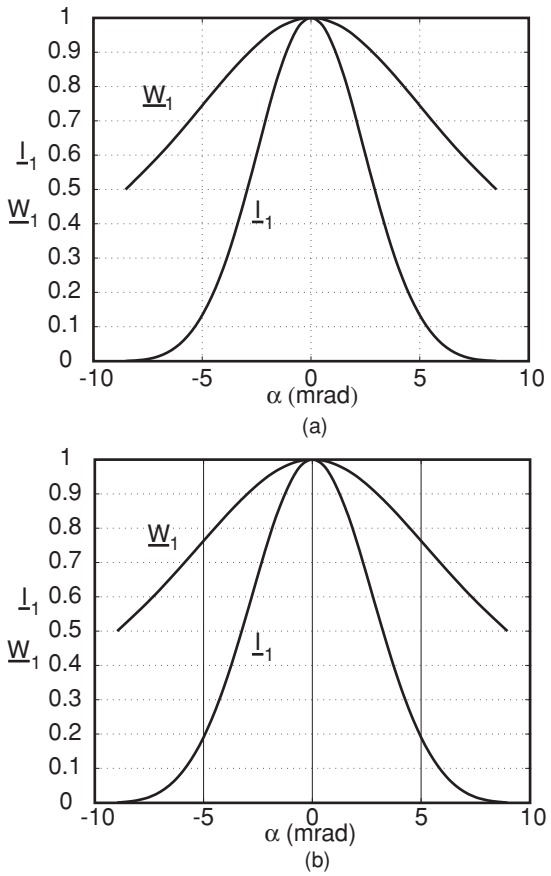

FIG. 9. Variations of intensity $\underline{I}_1$ and of quantum energy $\underline{W}_1$ with angle $\alpha = \pi - \theta$, normalized to maximum values, for two cases: (a) for $E_i = 60$ MeV, $\gamma_0 = 117.4$, $|\beta_0| = 0.999\,96$, $I_L = 3.454 \times 10^{17}$ Wm^{-2}, $E_{M1} = 1.613 \times 10^{10}$ Vm^{-1}, $\omega_L = 1.770 \times 10^{14}$ rad s^{-1}, $\phi' = 0$, $\eta_i = 0$, $a_1 = 0.053\,46$, $a_2 = 0$, and $W_{b1} = 6.42$ keV and (b) for $E_i = 57$ MeV, $\gamma_0 = 111.5$, $|\beta_0| = 0.999\,96$, $I_L = 8.661 \times 10^{20}$ Wm^{-2}, $E_{M1} = 8.078 \times 10^{11}$ Vm^{-1}, $\omega_L = 2.355 \times 10^{15}$ rad s^{-1}, $\phi' = 0$, $\eta_i = 0$, $a_1 = 0.2012$, $a_2 = 0$, and $W_{b1} = 77.08$ keV.

Moreover, the theoretical values of W_{b1}, the energy of the backscattered radiation, which is given by (114), is in good agreement with the experimental values from Refs. [17] and [18]. In the first case, we obtain $W_{b1} = 6.42$ keV, which corresponds, by virtue of (115), to the value $\lambda_{b1} = 1.93$ Å. This value matches the experimental value reported in Ref. [17], which is $\lambda_{b1\text{expt}} = 1.8$ Å. In the second case, we obtain $W_{b1} = 77.08$ keV, which matches the value $W_{b1\text{expt}} = 78.5$ keV, reported in Ref. [18].

We have proved in Sec. III B the existence of harmonics of the scattered radiation frequency in the system S' [see Eq. (101)]. An identical calculation, made for $j = 2$, leads to the the following expression of the second harmonic of the energy of the relativistic backscattered radiation:

$$W_{b2} = \omega_{b2}\hbar = 2\omega_L\gamma_0^2(1 + |\beta_0|)^2\hbar. \tag{131}$$

Recall that the fundamental energy $W_{b1} = \omega_L\gamma_0^2(1 + |\beta_0|)^2\hbar$ is given by Eq. (114). A recent experiment [34] proved the existence of the second harmonics. In that experiment, $E_i = 60$ MeV, $\gamma_0 = 117.4$, $\lambda_L = 10.6\,\mu$m, $\omega_L = 1.777 \times 10^{14}$ rad s^{-1}, and the laser beam is linearly polarized, corresponding to $a_1 = 0.35$. By using (114) and (131), we obtain the following values for the fundamental energy and for the second harmonic: $W_{b1} = 6.45$ keV and $W_{b2} = 12.9$ keV. The experimental values from the aforementioned experiment are, respectively, $W_{b1\text{expt}} = 6.5$ keV and $W_{b2\text{expt}} = 13$ keV, which are in good agreement with our theoretical values.

Our treatment, which leads to the existence of the harmonics, is based on the periodicity property, which has been proved in this paper. In Ref. [34], the demonstration of the existence of the second harmonic is completely different; it is based on the relativistic Doppler shift of the frequency.

IV. CONCLUSIONS

Starting from basic equations, we proved that the intensity of the Thomson scattered field in relativistic interactions between a very intense electromagnetic field and an electron is a periodic function of the phase of the incident field. Two consequences of this property result directly.

The first consequence is that the fundamental frequency of the scattered field is identical to the frequency of the incident field. Moreover, the periodicity property leads to the existence of harmonics, in the case of the backscattering of the electromagnetic fields on relativistic electrons, when the analysis is made in the inertial system in which the initial velocity of the electron is zero. These results are in good agreement with recent experimental measurements.

The second consequence is that the expressions of the intensity of the electrical scattered field and of the intensity of the scattered radiation can be put in the form of a composite function of only one variable, and it is not necessary to obtain explicit analytical expressions for these quantities. It results in the possibility of a very general treatment, in which we take into account all the parameters of the system such as the components of the initial velocity of the electron, the initial phase of the field, and both relativistic parameters when the field is elliptically polarized. Due to the fact that the treatment is general, a series of physical effects can be easily revealed. For example, when the initial velocity is not parallel to the wave vector of the incident field, then the lobes of the scattered beam become asymmetrical. Another example is as follows: When the component of the initial velocity in the negative direction of the oz axis increases, then the backscattered component also increases. Since the solution of the basic equations is exact, the theoretical results are in good agreement with numerous experimental data from literature.

ACKNOWLEDGMENTS

This work was done in the frame of the basic research program of the National Institute for Laser, Plasma and Radiation Physics, entitled "Nucleus Program."

APPENDIX: CONNECTION BETWEEN THE QUANTUM AND CLASSICAL EQUATIONS FOR THE SYSTEM DISCUSSED IN SECTION II

We show that the property which has been demonstrated by Motz and A. Selzer [35] results directly from a connection between Klein-Gordon and relativistic Hamilton-Jacobi equations, written for the system described in Sec. II A. The Klein-Gordon for this system is [44]

$$\left[c^2(-i\hbar\overline{\nabla}+e\overline{A})^2-\left(i\hbar\frac{\partial}{\partial t}\right)^2+(mc^2)^2\right]\Psi=0, \tag{A1}$$

where Ψ is the wave function. Recall that e is the absolute value of the electron charge.

With the substitution

$$\Psi=C\exp\left(\frac{i\sigma}{\hbar}\right), \tag{A2}$$

where C is an arbitrary constant and σ is a complex valued function of the electron coordinates and time, the Klein-Gordon equation (A1) becomes

$$c^2(\overline{\nabla}\sigma+e\overline{A})^2-\left(\frac{\partial\sigma}{\partial t}\right)^2+(mc^2)^2 - i\hbar c^2\left[\overline{\nabla}\cdot(\overline{\nabla}\sigma+e\overline{A})-\frac{\partial^2\sigma}{c^2\partial t^2}\right]=0. \tag{A3}$$

The relativistic Hamilton-Jacobi equation, written for the same system, is [36]

$$c^2(\overline{\nabla}S+e\overline{A})^2-\left(\frac{\partial S}{\partial t}\right)^2+(mc^2)^2=0. \tag{A4}$$

In Sec. II D, we proved Eq. (55), that is,

$$\overline{\nabla}\cdot(\overline{\nabla}S+e\overline{A})-\frac{\partial^2 S}{c^2\partial t^2}=0. \tag{A5}$$

By Eqs. (A2)–(A5), we obtain the following property: For a system composed of an electron interacting with a very intense electromagnetic field of a laser beam, the Klein-Gordon equation is verified by the wave function associated to the classical motion $C\exp(iS/\hbar)$, where S is the solution of the relativistic Hamilton-Jacobi equation, written for the same system.

We observe that the proof of this property does not use any approximation.

[1] N. Bloembergen, Proc. IEEE **51**, 124 (1963).
[2] Vachaspati, Phys. Rev. **128**, 664 (1962).
[3] L. S. Brown and T. W. B. Kibble, Phys. Rev. **133**, A705 (1964).
[4] E. S. Sarachik and G. T. Schappert, Phys. Rev. D **1**, 2738 (1970).
[5] A. K. Puntajer and C. Leubner, Phys. Rev. A **40**, 279 (1989).
[6] E. Esarey, S. K. Ride, and P. Sprangle, Phys. Rev. E **48**, 3003 (1993).
[7] I. Castillo-Herrera and T. W. Johnston, IEEE Trans. Plasma Sci. **21**, 125 (1993).
[8] S. K. Ride, E. Esarey, and M. Baine, Phys. Rev. E **52**, 5425 (1995).
[9] Y. I. Salamin and F. H. M. Faisal, Phys. Rev. A **54**, 4383 (1996).
[10] Y. I. Salamin and F. H. M. Faisal, Phys. Rev. A **55**, 3964 (1997).
[11] B. Shen *et al.*, Opt. Commun. **136**, 239 (1997).
[12] F. V. Hartemann, Phys. Plasmas **5**, 2037 (1998).
[13] S. P. Gorelavskii, S. V. Popruzhenko, and O. V. Shcherbachev, Laser Phys. **9**, 1039 (1999).
[14] F. He, Y. Y. Lau, D. P. Umstadter, and T. Strickler, Phys. Plasmas **9**, 4325 (2002).
[15] Y. Y. Lau, F. He, D. P. Umstadter, and R. Kowalczyk, Phys. Plasmas **10**, 2155 (2003).
[16] S. Bannerjee *et al.*, J. Opt. Soc. Am. B **20**, 182 (2003).
[17] I. V. Pogorelsky *et al.*, Phys. Rev. Spec. Top.–Accel. Beams **3**, 090702 (2000).
[18] S. G. Anderson *et al.*, Appl. Phys. B: Lasers Opt. **78**, 891 (2004).
[19] K. J. Kim, S. Chattopadhay, and C. V. Shank, Nucl. Instrum. Methods Phys. Res., Sect. A **341**, 351 (1994).
[20] D. Umstadter, Phys. Lett. A **347**, 121 (2005).

[21] P. Tomassini, A. Giulietti, D. Giulietti, and L. A. Gizzi, Appl. Phys. B: Lasers Opt. **80**, 419 (2005).
[22] H. Kotaki, P. Tomassini, A. Giulietti, D. Giulietti, and L. A. Gizzi, Nucl. Instrum. Methods Phys. Res., Sect. A **455**, 166 (2000).
[23] I. Sakai *et al.*, Phys. Rev. Spec. Top.–Accel. Beams **6**, 091001 (2003).
[24] H. Schwoerer, B. Liesfeld, H.-P. Schlenvoigt, K.-U. Amthor, and R. Sauerbrey, Phys. Rev. Lett. **96**, 014802 (2006).
[25] C. Bula *et al.*, Phys. Rev. Lett. **76**, 3116 (1996).
[26] P. Panek, J. Z. Kaminski, and F. Ehlotzky, Phys. Rev. A **65**, 022712 (2002).
[27] L. Dongguo, K. Yokoya, T. Hirose, and R. Hamatsu, Jpn. J. Appl. Phys. **42**, 5376 (2003).
[28] Y. Yorozu *et al.*, Appl. Phys. B: Lasers Opt. **76**, 293 (2003).
[29] C. Harvey, T. Heinzl, and A. Ilderton, Phys. Rev. A **79**, 063407 (2009).
[30] M. Boca and V. Florescu, Phys. Rev. A **80**, 053403 (2009).
[31] J. D. Jackson, *Classical Electrodynamics* (Wiley, New York, 1999).
[32] V. B. Berestetskii, E. M. Lifshitz, and L. P. Pitaevskii, *Quantum Electrodynamics*, 2nd ed. (Pergamon, New York, 1982).
[33] J. Meyer-ter-vehn and A. Pukhov, *Atoms, Solids and Plasmas in Super Intense Laser Fields* (Plenum, New York, 2001).
[34] M. Babzien *et al.*, Phys. Rev. Lett. **96**, 054802 (2006).
[35] L. Motz and A. Selzer, Phys. Rev. **133**, B1622 (1964).
[36] L. D. Landau and E. M. Lifshitz, *The Classical Theory of Fields* (Pergamon, London, 1959).
[37] D. Marcuse, *Engineering Quantum Electrodynamics* (Harcourt, Brace and World, New York, 1970).
[38] S. Y. Chen, A. Maksimchuk, and D. Umstadter, Nature (London) **396**, 653 (1998).
[39] G. A. Mourou, T. Tajima, and S. V. Bulanov, Rev. Mod. Phys. **78**, 309 (2006).
[40] M. Abadi and L. Lamport, ACM Trans. Program. Languages Syst. **15**, 73 (1993).
[41] See Supplemental Material at http://link.aps.org/supplemental/10.1103/PhysRevA.84.023824, for containing the MATHEMATICA 7 scripts used in the paper.
[42] K. Ta Phuok, F. Burgy, J.-P. Rousseau, and A. Rousse, Eur. Phys. J. D **33**, 301 (2005).
[43] W. Heitler, *The Quantum Theory of Radiation* (Clarendon, Oxford, 1960).
[44] A. Messiah, *Quantum Mechanics* (North-Holland, Amsterdam, 1965), Vol. 2.